Quantum vortices leave a macroscopic signature in the thermal background

Luca Galantucci,[1,2,*] Giorgio Krstulovic,[3,†] and Carlo F. Barenghi[2,‡]
[1] Istituto per le Applicazioni del Calcolo M. Picone, IAC-CNR, Via dei Taurini 19, Roma 00185, Italy
[2] School of Mathematics, Statistics and Physics, Newcastle University, Newcastle upon Tyne NE1 7RU, United Kingdom
[3] Université Côte d'Azur, Observatoire de la Côte d'Azur, CNRS, Laboratoire
J. L. Lagrange, Boulevard de l'Observatoire CS 34229 - F 06304 NICE Cedex 4, France
(Dated: October 25, 2025)

Supplementary Material

Methods

The FOUCAULT model. Our model considers the the superfluid as a collection $\mathcal{L}$ of vortex lines that advect each other following Biot-Savart integrals. Vortex lines are parametrised employing arclength ξ and time t, *i.e.* the position of the vortex filaments is given by $\mathbf{s}(\xi, t)$. Regularisation of the integrals and reconnections are built following the Schwarz's vortex filament model [1]. The vortex lines interact with the normal fluid through mutual friction coefficients β and β' as follows

$$\mathbf{v}_L = \dot{\mathbf{s}}(\xi, t) = \frac{\partial \mathbf{s}}{\partial t} = \mathbf{v}_{\mathrm{s}_\perp} + \beta \mathbf{s}' \times \mathbf{v}_{\mathrm{ns}} - \beta' \mathbf{s}' \times (\mathbf{s}' \times \mathbf{v}_{\mathrm{ns}}), \quad (1)$$

where $\mathbf{s}' = \partial \mathbf{s}/\partial \xi$ is the unit tangent vector, the subscript '$\perp$' indicates the component of the superfluid velocity lying on a plane orthogonal to $\mathbf{s}'$ and $\mathbf{v}_{\mathrm{ns}} = \mathbf{v}_{\mathrm{n}} - \mathbf{v}_{\mathrm{s}}$ at $\mathbf{s}$, with $\mathbf{v}_{\mathrm{s}}$ the superfluid velocity given by the Biot-Savart integral

$$\mathbf{v}_{\mathrm{s}}(\mathbf{s}, t) = \overline{\mathbf{v}}_{\mathrm{s}} + \frac{\kappa}{4\pi} \oint_{\mathcal{L}} \frac{\mathbf{s}'(\xi, t) \times (\mathbf{s} - \mathbf{s}(\xi, t))}{|\mathbf{s} - \mathbf{s}(\xi, t)|^3} d\xi. \quad (2)$$

In turn, the normal fluid satisfies the incompressible Navier-Stokes equations

$$\frac{\partial \mathbf{v}_{\mathrm{n}}}{\partial t} + (\mathbf{v}_{\mathrm{n}} \cdot \nabla)\, \mathbf{v}_{\mathrm{n}} = -\frac{1}{\rho} \nabla p_{\mathrm{n}} + \nu_{\mathrm{n}} \nabla^2 \mathbf{v}_{\mathrm{n}} + \frac{\mathbf{F}_{\mathrm{ns}}}{\rho_{\mathrm{n}}} \quad (3)$$

$$\mathbf{F}_{\mathrm{ns}} = \oint_{\mathcal{L}} \mathbf{f}_{\mathrm{ns}}(\mathbf{s}) \delta(\mathbf{x} - \mathbf{s}) \mathrm{d}\xi \ , \quad \nabla \cdot \mathbf{v}_{\mathrm{n}} = 0 \ . \quad (4)$$

where $\mathbf{F}_{\mathrm{ns}}$ is mutual friction force per unit volume responsible for the retroaction of quantum vortices on $\mathbf{v}_{\mathrm{n}}$, and

$$\mathbf{f}_{\mathrm{ns}}(\mathbf{s}) = -D\, \mathbf{s}' \times [\mathbf{s}' \times (\dot{\mathbf{s}} - \mathbf{v}_n(\mathbf{s}))] - \rho_n \kappa\, \mathbf{s}' \times (\dot{\mathbf{s}} - \mathbf{v}_n(\mathbf{s})) \quad (5)$$

its local density, where D is a friction coefficient [2]. The second term in equation 5 is the Iordanskii force: this term is responsible for the misalignment of the direction of the relative velocity between the vortex and the normal fluid (indicated by the ruler in Fig. 3 (left) of the main text and in Fig. S1 (left)) and the axis of the wake. The total density of liquid helium is $\rho = \rho_{\mathrm{n}} + \rho_{\mathrm{s}}$, with ρ_{n} and ρ_{s} are respectively the normal fluid and superfluid densities. Finally, p_{n} is the effective pressure, and ν_{n} the kinematic viscosity of the normal fluid. The mean normal fluid velocity $\overline{\mathbf{v}}_{\mathrm{n}}$ is directly imposed during the evolution.

A complete description of the Fully cOUpled loCAl model of sUperfLuid Turbulence (FOUCAULT), including its numerical implementation, can be found in [2].

Numerical details. The Navier-Stokes equations are solved in a periodic domain using a standard pseudo-spectral code. In all simulations we use a grid of 512^3 grid points. The vortex filament model is evolved using a Tree-Algortihm method that allows for an important speed up of the Biot-Savart computations. The number of discretisation points used to represent the vortex lines is adapted during the simulations, and fluctuates in the steady state around 700 and 10^4 for $v_{ns}^{(1)}$ and $v_{ns}^{(2)}$, respectively.

Single vortex wake at $v_{ns} = v_{ns}^{(2)}$ =0.94 cm/s

The pattern of the normal fluid past a single vortex at counterflow velocity $v_{ns} = v_{ns}^{(1)} = 0.27$ cm/s was shown in Fig. 3 of the main text. For completeness, Fig. S1 displays the wake generated by a single, straight superfluid vortex oriented in the positive y-direction in the presence of counterflow in the z-direction at counterflow velocity $v_{ns} = v_{ns}^{(2)} = 0.94$cm/s at $t \approx \tau_r/10$. In the left panel, we report the relative normal fluid streamwise velocity fluctuations $\Delta v_n^z = \delta v_n^z/\bar{v}_n^z = (v_n^z(x,z) - \bar{v}_n^z)/\bar{v}_n^z$ vs x and z at fixed y_0. In the centre (right) panel we report the PDFs of the streamwise (spanwise) normal fluid velocity fluctuations δv_n^z (δv_n^x). With respect to the spanwise (x) fluctuations (Fig. S1, right), the PDF has been computed taking also into account the fluctuations generated by a vortex oriented in the negative y-direction (this is not necessary for the streamwise component as in this circumstance the fluctuations generated coincide).

Calculation of wake size in the single vortex simulation

For both counterflow velocities $v_{ns}^{(1)}$ and $v_{ns}^{(2)}$ we compute the size of the wake at $t \approx \tau_r/10$, employing the two-dimensional normal fluid velocity field resulting from the motion of a single, straight superfluid vortex in presence of a counterflow. The corresponding relative streamwise velocity fluctuations $(v_n^z(x,z) - \bar{v}_n^z)/\bar{v}_n^z$ have been reported in Fig. 3 (left) in the main text and Fig. S1 (left) in the

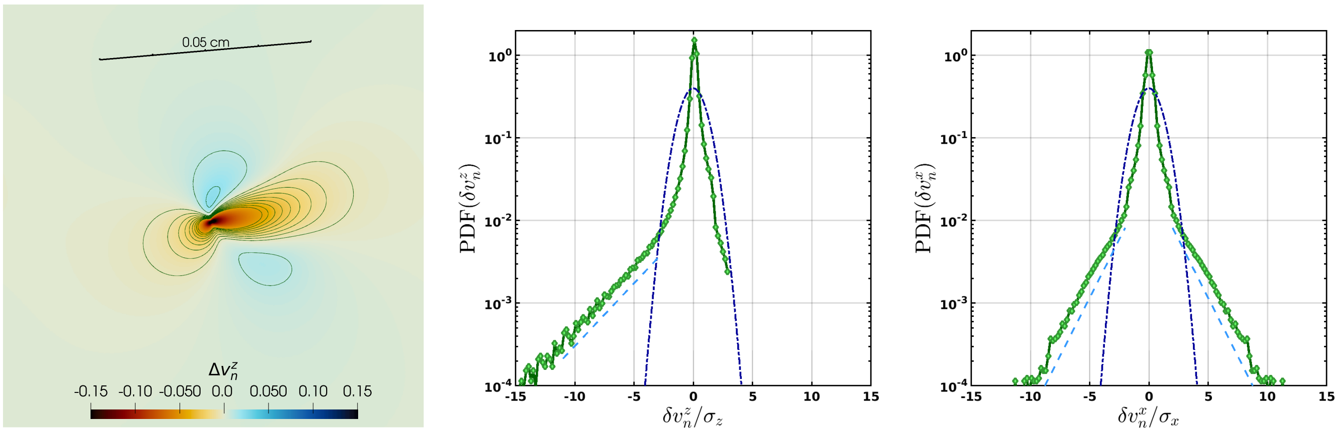

Fig. S1 Single vortex wake. Temperature $T = 1.5$ K and $v_{ns}^{(2)} = 0.94$cm/s Left column: relative normal fluid streamwise velocity fluctuations $\Delta v_n^z = \delta v_n^z/\bar{v}_n^z = (v_n^z(x,z) - \bar{v}_n^z)/\bar{v}_n^z$ vs x and z at fixed y_0. The ruler indicates the direction of the relative velocity of the single vortex line with respect to the normal fluid. Centre column: PDF(δv_n^z) vs $\delta v_n^z/\sigma_z$, where $\delta v_n^z = v_n^z - \bar{v}_n^z$ and σ_z is the standard deviation. Right column: PDF(δv_n^x) vs $\delta v_n^x/\sigma_x$, where $\delta v_n^x = v_n^x$ ($\bar{v}_n^x = 0$) and σ_x is the standard deviation. Gaussian distributions are showed in dot-dashed dark blue line for reference. The dashed cyan lines are exponential functions to guide the eye.

Supplementary Information for $v_{ns}^{(1)}$ and $v_{ns}^{(2)}$, respectively. The size of the wake, w, is defined as follows:

$$w = \sqrt{\frac{\int_{\mathcal{S}} |\mathbf{x} - \mathbf{s}_0|^2 |\delta\tilde{\mathbf{v}}_n|^2 dxdz}{\int_{\mathcal{S}} |\delta\tilde{\mathbf{v}}_n|^2 dxdz}} \,, \tag{6}$$

where $\mathcal{S}$ is the x-z two-dimensional domain orthogonal to the superfluid vortex at fixed y_0 (i.e. the domain reported in Fig. 3 (left) in the main text and Fig. S1 (left) in the Supplementary Information); $\mathbf{x} = (x, z)$ is the general position vector; $\mathbf{s}_0$ is the intersection of the vortex with $\mathcal{S}$ at $t \approx \tau_r/10$; $\delta\tilde{\mathbf{v}}_n = (v_n^x, v_n^z - \bar{v}_n^z)$.

Oseen solution

In two-dimensions, the Stokes equation describing the steady flow of a viscous fluid past a circle at low Reynolds number has no solution: it is impossible to enforce simultaneously a no-slip boundary condition on the circle and the condition of uniform flow at infinity (Stokes'paradox). In order to determine the flow of the fluid, it is necessary to employ Oseen's equation [3] which includes a linearised convective term. With reference to Fig. S2, the velocity of the viscous fluid $\mathbf{V}$ can be expressed in terms of the velocity of the fluid at infinity $\mathbf{U}$ and a perturbation $\mathbf{v}$, as follows $\mathbf{V} = \mathbf{U} + \mathbf{v}$, where $\mathbf{U} = U\hat{\mathbf{k}}$, $\hat{\mathbf{k}}$ being the unit vector in the z (horizontal) direction (x is the vertical direction). At large distances $r \gg a_0$, the distances we are interested in, $\mathbf{V} \approx \mathbf{U}$ (or, equivalently, $v \ll U$) and hence the convective term may be approximated as follows, $(\mathbf{V}\cdot\nabla)\mathbf{V} \approx U\frac{\partial}{\partial z}\mathbf{v}$ leading to the Oseen equation for the perturbation $\mathbf{v}$:

$$U\frac{\partial}{\partial z}\mathbf{v} = -\frac{1}{\rho}\nabla p + \nu\nabla^2\mathbf{v}. \tag{7}$$

The normalised far field solution $\mathbf{v}' = \mathbf{v}/U$ of equation (7), *i.e.* the solution for $r \gg a_0/Re$, is, in polar coordinates, given by the following expressions [3]

$$v_r' = \frac{C_0}{2}\sqrt{\frac{\pi}{\tilde{r}}}\,(1+\cos\theta)\,e^{-\frac{\tilde{r}}{2}(1-\cos\theta)} - \frac{C_0}{\tilde{r}},$$
$$v_\theta' = -\frac{C_0}{2}\sqrt{\frac{\pi}{\tilde{r}}}\sin\theta\, e^{-\frac{\tilde{r}}{2}(1-\cos\theta)} \,, \tag{8}$$

where $\tilde{r} = r\frac{Re}{a_0}$ is the Oseen non-dimensional variable (the far field corresponds to $\tilde{r} \gg 1$),

$$C_0 = -\frac{2}{0.5 - \gamma - \log(\epsilon/2)}, \tag{9}$$

$\gamma = 0.5772$ is the Euler-Mascheroni constant and $v' = v/U$. The resulting far-field vorticity ω is given by the following expression

$$\omega = \frac{C_0 Re}{2}\sin\theta e^{-\frac{\tilde{r}}{2}(1-\cos\theta)}\sqrt{\frac{\pi}{\tilde{r}}} \,, \tag{10}$$

whose spatial dependence is reported in Fig. S3. It is important to note the upstream/downstream asymmetry.

The far field solution of Oseen's equation (8) can be employed to determine the spatial dependence of the flow in the far wake, *i.e.* for $\tilde{r} \gg 1$ and $\theta \ll 1$. In this region the flow is described by the following expressions

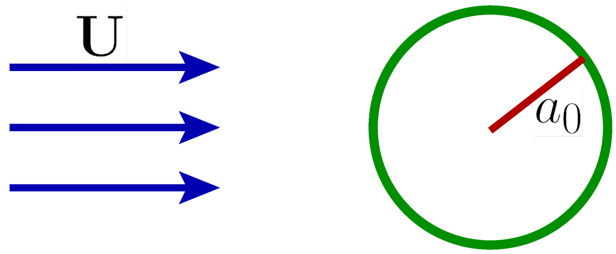

Fig. S2 Schematic rendering of the two-dimensional flow past a circle.

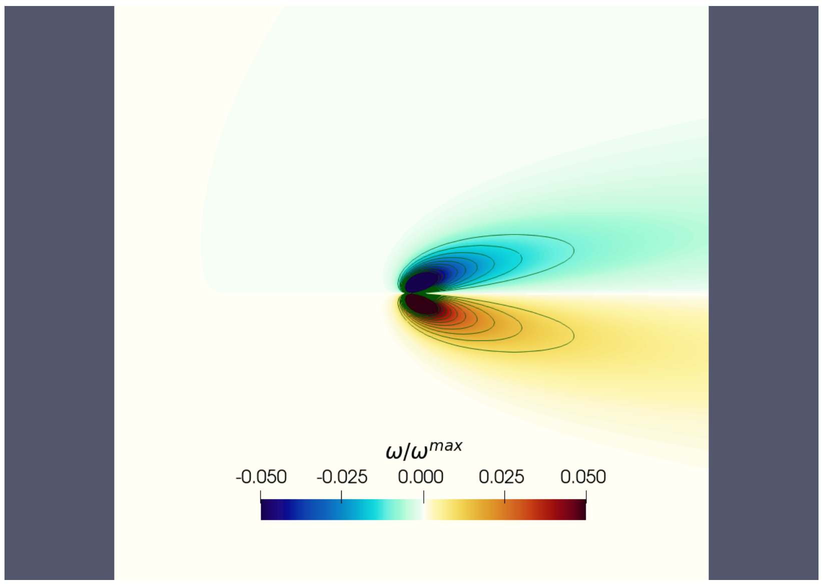

Fig. S3 Far field Oseen solution: vorticity field normalised by its maximum value ω/ω_{max}. The size of the domain is 0.1 cm.

$$v'_r = C_0\sqrt{\frac{\pi}{\tilde{r}}}\, e^{-\frac{\tilde{r}\theta^2}{4}} - \frac{C_0}{\tilde{r}},$$

$$v'_\theta = -\frac{C_0}{2}\sqrt{\frac{\pi}{\tilde{r}}}\theta\, e^{-\frac{\tilde{r}\theta^2}{4}} \ , \tag{11}$$

whose streamwise component $v'^z = (V^z - U)/U$ is reported in Fig. S4. The iso-lines in Fig. S4 are drawn at the same values of the relative magnitude of streamwise velocity fluctuations employed in Fig. 3. If we compare the linear sizes of the wakes ($e.g$ the linear size of the region where $v'^z < -0.05$) we find very good agreement between the analytical solution of Oseen's equation and our numerical results. Furthermore, if we compute the PDFs of the streamwise and spanwise velocity fluctuations, v^z and v^x, respectively reported in Fig. S5 (left) and (right), in the far wake (for $\tilde{r} > 10$ and $\theta < 10°$), we recover the same characteristics observed for the normal fluid velocity in our counterflow turbulence simulations and in the analysis of the single vortex wake: the PDFs are skewed and/or with exponential tails. This similarity supports our conclusion that the normal fluid in a turbulent helium counterflow is the superposition of a uniform background flow generated by the heater and flow disturbances (consisting of small vortex dipoles and large almost parabolic wakes) generated by the vortices via the friction force.

Skewness of vortex velocity $\mathbf{v}_L$

Consider equation (1) in the **Methods** section. For $T \geq 1.5$K (the temperature range where the $\rho_n/\rho > 0.1$) we have $|\beta'| > \beta > 0$, hence the streamwise vortex velocity v_L^z can be written as follows:

$$\begin{aligned} v_L^z(\mathbf{s}) &= (1-|\beta'|)(\bar{v}_s^z + v_{_{BS}}^z(\mathbf{s})) + |\beta'| v_n^z(\mathbf{s}) \\ &= \varepsilon_1(\bar{v}_s^z + v_{_{BS}}^z(\mathbf{s})) + \varepsilon_2 v_n^z(\mathbf{s}) \ , \end{aligned} \tag{12}$$

where $v_{_{BS}}^z(\mathbf{s})$ is the streamwise component of the Biot-Savart integral in equation (2) in the **Methods** section, $\varepsilon_1 = 1 - |\beta'| = 0.88$, $\varepsilon_2 = |\beta'| = 0.12$, $\varepsilon_1 + \varepsilon_2 = 1$, ε_1 and ε_2 depend on temperature T and Reynolds number and as temperature increases $\varepsilon_1 \to 0$ and $\varepsilon_2 \to 1$. Values of ε_1 and ε_2 reported are evaluated at $T = 1.5$K [2], and the velocities $v_{_{BS}}^z$ and v_n^z are evaluated on the vortex positions $\mathbf{s}$.

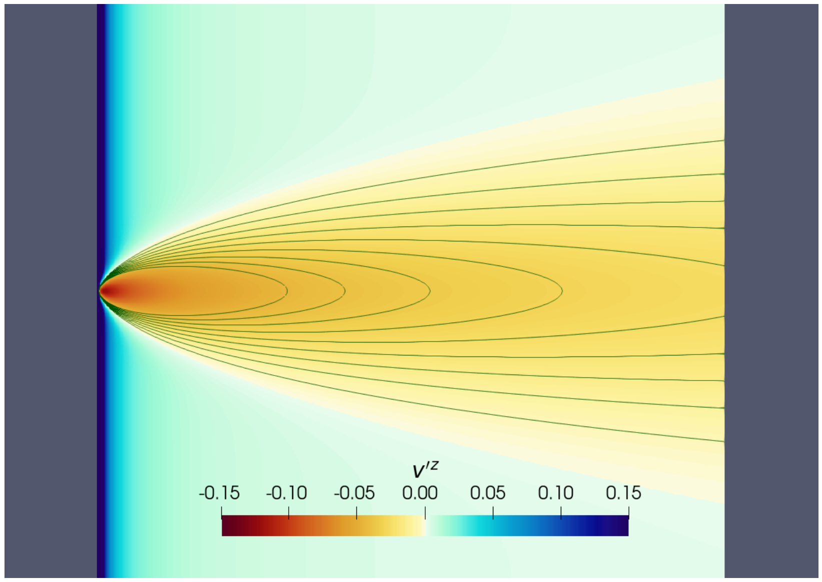

Fig. S4 Far Wake Oseen solution: relative magnitude of the streamwise velocity fluctuations $v'^z = v^z/U = (V^z - U)/U$. The size of the domain is 0.1 cm. Iso-lines are drawn at the same values as in Figs. 3 and S1.

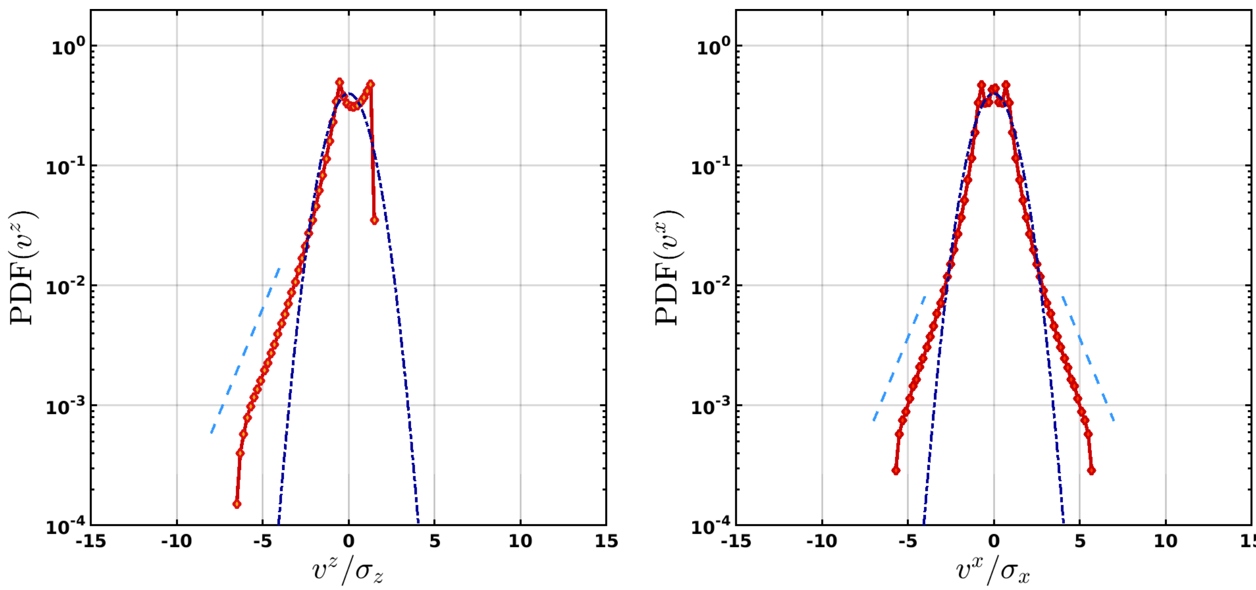

Fig. S5 Far wake Oseen solution: Left: PDF(v^z) vs v^z/σ_z, where v^z is the streamwise velocity fluctuation of the solution of Oseen's equation in the far wake region and σ_z is the standard deviation. Right: PDF(v^x) vs v^x/σ_x, where v^x is the spanwise velocity fluctuation of the solution of Oseen's equation in the far wake region and σ_x is the standard deviation. Gaussian distributions are showed in dot-dashed dark blue line for reference. The dashed cyan lines are exponential functions to guide the eye.

Equation (12) implies that, in the first approximation, the streamwise vortex velocity fluctuation δv_L^z has the following expression:

$$\delta v_L^z(\mathbf{s}) = \varepsilon_1 \delta v_{_{BS}}^z(\mathbf{s}) + \varepsilon_2 \delta v_n^z(\mathbf{s}) \tag{13}$$

To quantify the asymmetry of the PDF of δv_L^z (reported in Fig. 4 and echoing the experimental non symmetric distribution of the streamwise velocity of particles likely trapped on vortices [4]), the relevant quantity to compute is the skewness of v_L^z defined as $\mathcal{S}(v_L^z) = \overline{[\delta v_L^z(\mathbf{s})]^3}$ which, following equation (13), depends on $\mathcal{S}(v_{_{BS}}^z)$, $\mathcal{S}(v_n^z)$ and other velocity cross correlation terms. For $v_{ns} = v_{ns}^{(2)} = 0.94$ cm/s (as experiments in Ref.[4] are performed at large v_{ns}) we obtain the following values for the skewnesses (in non-dimensional units scaled with unit of length $\lambda = 1.59\times10^{-2}$cm and unit of time $\tau = 1.22\times10^{-2}$s): $\mathcal{S}(v_L^z) = -2.3\times10^{-4}$, $\mathcal{S}(v_{_{BS}}^z) = -1.8\times10^{-4}$ and $\mathcal{S}(v_n^z) = -8\times10^{-4}$. Hence, the skewness of $v_{_{BS}}^z$ does not fully account for the skewness of v_L^z, implying that the skewness of v_n^z arising from the existence of the wakes, contributes to $\mathcal{S}(v_L^z)$ and hence to the non symmetrical character of the statistical distributions of the velocity of inertial particles observed in experiments [4]. As ε_2 increases for increasing temperature, the impact of the wakes on the experimental particle velocity statistics is likely to increase with temperature.

References

* luca.galantucci@cnr.it
† giorgio.krstulovic@oca.eu
‡ carlo.barenghi@newcastle.ac.uk

1. K. W. Schwarz, Phys. Rev. B **38**, 2398 (1988).
2. L. Galantucci, A. Baggaley, C. Barenghi, and G. Krstulovic, Eur. Phys. J. Plus **135**, 547 (2020).
3. H. Lamb, Cambridge University Press , 1 (1932).
4. P. Švančara, D. Duda, P. Hrubcová, M. Rotter, L. Skrbek, M. La Mantia, E. Durozoy, P. Diribarne, B. Rousset, M. Bourgoin, *et al.*, J. Fluid Mech. **911**, A8 (2021).